Journal of Chromatography A, 1226 (2012) 116–123

Contents lists available at SciVerse ScienceDirect

Journal of Chromatography A

journal homepage: www.elsevier.com/locate/chroma

A reversed-flow differential flow modulator for comprehensive two-dimensional gas chromatography

James F. Griffith[a], William L. Winniford[a,*], Kefu Sun[a], Rob Edam[b], Jim C. Luong[c]

[a] The Dow Chemical Company, 2301 N. Brazosport Blvd, Freeport, TX 77541-3257, USA
[b] Dow Benelux, Terneuzen, The Netherlands
[c] Dow Canada, Fort Saskatchewan, Alberta, Canada

ARTICLE INFO

Article history:
Available online 4 December 2011

Keywords:
GC × GC
Comprehensive two-dimensional gas chromatography
Fragrance
Differential flow modulation
Pulsed flow modulation

ABSTRACT

A simple and reliable differential flow modulator has been demonstrated which reverses the flow during the flush step. The modulator is constructed with commercially available capillary flow technology tees which simplifies the apparatus and permits wide range of column dimensions to be used because the modulator volume is adjustable. Using a reverse flush arrangement the tailing of the peak at the base (baseline rise between modulations) is reduced 10–20 fold as compared to forward flush modulation. This is most easily observed for peaks overloaded in the first dimension. Excellent reproducibility (<2% RSD) of area measurements has been demonstrated with a complex fragrance sample as well as the capacity to handle significant overloading without loss of resolution in the second dimension. Further demonstrating the flexibility of this modulator, separation of C1–6 alkanes and olefins are demonstrated with two porous layer open tubular columns.

1. Introduction

Differential flow (or pulsed flow) modulation for comprehensive two-dimensional gas chromatography, based on Deans switching, was first described by Bueno and Seeley [1]. After demonstrating the utility of this modulator in two publications [2,3], Seeley developed a much simpler version that required only two tees and a solenoid valve to control the Deans switch [4]. Subsequent papers by Kochman et al. [5], Seeley and co-workers [6–9], Poliak et al. [10], Gu et al. [11], Semard et al. [12], and Manzano et al. [13] further demonstrated the utility of this technique. Tranchida et al. [14] made a custom built metal disk compromising of both a 3-port and 4-port Tee to give flexibility in the ratio of flows between column 1 and the flow flushing the modulator. Tranchida has also done a very thorough review and comparison of flow modulation versus thermal modulation [15]. As compared to other forms of modulation for GC × GC, differential flow modulation is desirable because of the operational simplicity and capability to successfully modulate components over the entire volatility range addressable by gas chromatography. Semard et al. [12] compared the peak capacity obtained with differential flow modulators and cryogenic modulators demonstrating that under the right conditions it is possible to get comparable results with the two techniques, though with very different column combinations. Because the second dimension peak capacity is not very large it is essential to eliminate any factors that would reduce or impair that separation. Quite often it is apparent that high concentration peaks overload and the 2D plot shows a solid streak in the second dimension at specific first dimension times. At first we accepted this as inevitable but it raised the question of whether it would be possible to have a component elute at high concentration and fully resolve it from coeluting trace components in the second dimension.

We have used the simplified differential flow modulator design [4], constructed with Valco tees, for several years in industrial laboratories. Changing columns is not trivial because each column is inserted through the respective tee to protrude into the accumulation capillary as shown in Fig. 1. This creates a pressure restriction that is important to the performance of the modulator. The complexity of the column and tee connections has restricted the application of this form of GC × GC to skilled operators. It also restricts the combinations of column diameters that can be used with the modulator capillary. For any technique to proliferate beyond the use of highly skilled practitioners it must be both simple and reliable. The introduction of aluminum ferrules has been essential in advancing this technique because they provide connections that remain tight even after temperature cycling, unlike Vespel/graphite ferrules which gradually loosen and leak. Capillary flow technology (CFT) tees have also facilitated connections with very little dead volume. Agilent has introduced the G8436A CFT modulator that facilitates the set up of GC × GC. However, it has a

* Corresponding author. Tel.: +1 979 238 9783; fax: +1 979 238 0715.
E-mail address: wlwinniford@dow.com (W.L. Winniford).

0021-9673/$ – see front matter © 2011 Elsevier B.V. All rights reserved.
doi:10.1016/j.chroma.2011.11.036

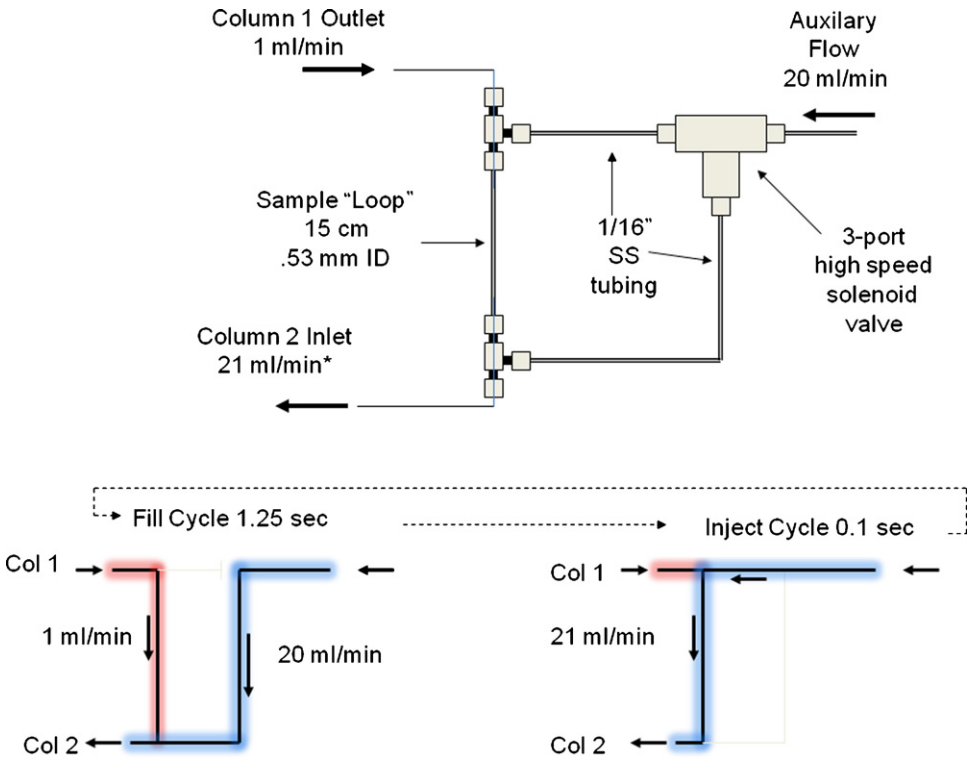

Fig. 1. Flow path of a differential flow modulator with forward fill/flush (FFF).

fixed internal loop and thus is somewhat limited in the combination of column internal diameters that can be used effectively.

Flow modulation as previously described and shown in Fig. 1 must be precisely timed so that the accumulation capillary is not overfilled during the fill cycle and is completely flushed during the short flush cycle. Otherwise the detector signal will not completely return to baseline between modulations of a peak, which in turn produces streaking and loss of resolution in the second dimension. To preserve resolution in the first dimension, the second dimension modulation period must be very short as described by Blumberg [16]. This in turn places demands on the injection bandwidth delivered to the second dimension column. The ratio of the modulation period (fill time + flush time) to the flush time determines how many peaks can be potentially resolved in the second dimension of any first dimension time slice. In practice we have found that the peak widths of the modulated peaks are much larger than predicted, especially as the absolute amount of a given component injected increases. With both the Agilent CFT modulator and an equivalent modulator constructed with two CFT tees and an external capillary, tailing becomes significant when larger quantities are injected. This effect is typically not seen with examples like gasoline or diesel samples where the amount of any single component is relatively small and the sample is injected with a high split ratio.

In the work by Semard et al. [12] a 100 μm ID first dimension column was used with a flow of 0.2 ml/min, making it possible to use an 11 second modulation period. With that tremendous gain in second dimension peak capacity, the first dimension column was operated at well below the optimum velocity giving up much of the potential efficiency and resolving power. Less obvious is that range of concentrations that can be handled without overloading the first dimension column has been substantially reduced. Investigations on catalyst poisons, odor or color bodies typically require sub ppm detection for common industrial samples. With such samples it is very common to inject mixtures that have one or more components at very high concentration, >10%, and low injection split ratios, <20/1. This means that the amount of a component delivered to the second dimension can be higher than 10 ng in some modulations to the second dimension. Because any tailing significantly reduces resolution in the second dimension and is detrimental to quantitation, we have investigated modifications that will narrow the peak width at the base and reduce the baseline rise between modulations onto the second dimension column. Most authors state peak widths at half height because it is far easier than measuring peak widths at the base. But in GC × GC separations any tailing in the second dimension substantially reduces the number of peaks resolved in the second dimension. In this article we describe a very simple and reliable modification, reversing the flow during modulation which substantially reduces tailing at the base of the second dimension peaks, reducing the baseline rise between modulations and effectively increasing the number of peaks that can be resolved in the second dimension. It also has the advantage that it can accommodate a very wide range of column dimensions.

2. Experimental

The reverse fill/flush modulator was constructed using 2-way non-purged splitter and 2-way purged splitter CFT plates (Agilent Technologies, Little Falls, DE, USA) as shown in Fig. 2. The sample accumulation "loops" were constructed from both fused silica tubing and SilcoSteel tubing (Restek, Bellefonte, PA, USA), dimensions are noted in Tables 1 and 2. A programmable logic controller (OMRON 10C1DR-D-V2 24VDC, Kyoto, Japan) was used to control the 3-way solenoid valve (Parker model 009-933-900 24VDC, Cleveland, OH, USA). These components were set up in an Agilent 7890 GC equipped with a split/splitless inlet and dual flame ionization detectors. Flow for the second dimension column was supplied by an auxiliary electronic pressure control (EPC) with no internal restriction. The operating conditions for the reverse flush/fill modulator experiments are given in Table 1. To replicate the experiments in forward fill/flush modulation the outlet of column 1 was

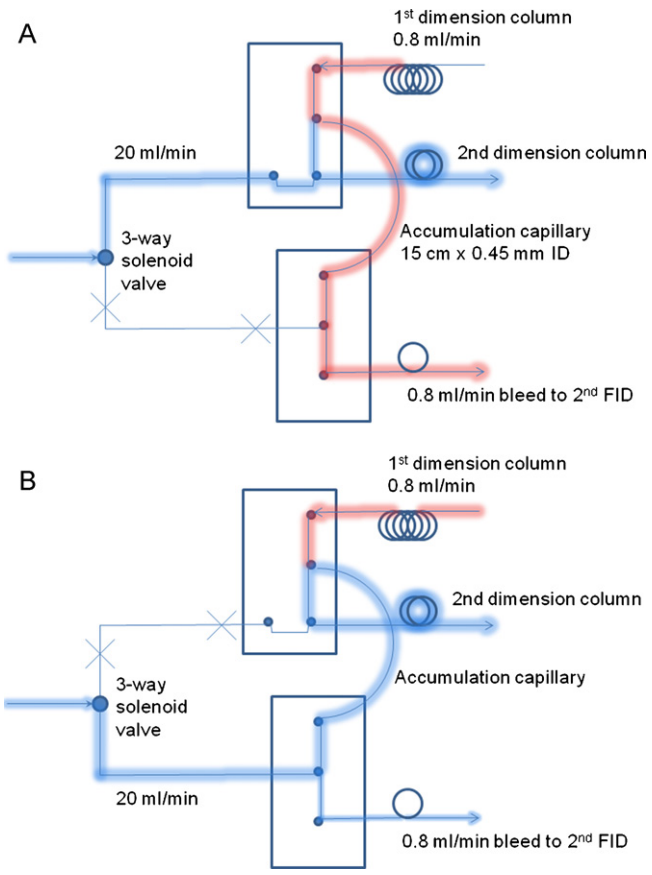

Fig. 2. (A) Reverse fill/flush (RFF) modulator: flow path of fill cycle. (B) Reverse fill/flush (RFF) modulator: flow path of flush cycle.

Table 1
Reversed fill/flush experimental conditions.

Loop dimensions: 15 cm × 0.45 cm ID SilcoSteel, 23.8 μl volume
First dimension column: DB5-MS ultrainert, 20 m × 0.18 mm ID × 0.36 μm film
First dimension flow: 0.8 ml/min H2, 23 psi @ 50 °C, constant flow mode
Second dimension column: DB-Wax, 5 m × 0.25 mm ID × 0.15 μm film
Second dimension flow: 20 ml/min H2, 16.5 psi @ 50 °C, constant flow mode
Fill time (exp opt): 1.2 s
Flush time (exp): 0.1 s
Bleed capillary: 3.2 m × 0.1 mm ID
Injector: 280 °C, injection volume and split ratio as noted in text
Oven temperature program: 50 °C, 1 min, 7 °C/min to 240 °C
FID Flows: H2 20 ml/min, air 400 ml/min, N2 makeup 40 ml/min

connected to the bottom port of the lower tee (in place of the bleed capillary) and the top port of the upper tee was capped. The only other change to the conditions given in Table 1 is that the flush time was lengthened to 0.13 s according to the optimization studies discussed later. For the example with PLOT columns an Agilent Low Thermal Mass (LTM) oven accessory was used to independently control the temperature of the second dimension column. Experimental conditions for the PLOT columns are given in Table 2. Note that for all experiments the FID hydrogen flow was set to 20 ml/min, with an additional 20 ml/min coming from the second dimension column. In all experiments both the first and second dimensions were operated in constant flow mode. Data was collected at 200 Hz with Agilent Chemstation software, rev B.04.02. 1D processing was done with the Agilent Chemstation software and 2D processing was done with GC-Image 2.1 data visualization software (Zoex Corp, Houston, TX, USA).

Table 2
Reversed fill/flush PLOT column experimental conditions.

Loop dimensions: 23 cm × 0.53 cm ID SilcoSteel, 50 μl volume
First dimension column: GasPro, 13.5 m × .25 mm ID
First dimension flow: 0.8 ml/min H2, 15.3 psi @ 50 °C, constant flow mode
Second dimension column: PoraBond Q, 2 m × 0.25 mm ID
Second dimension flow: 20 ml/min H2, 13.8 psi @ 50 °C, constant flow mode
Fill time (exp opt): 2.4 s
Flush time (exp): 0.2 s
Bleed capillary: 1.75 m × 0.1 mm ID
Oven program: 50 °C for 1 min, then 7 °C/min to 240 °C for 3.857 min
LTM oven program: 70 °C, 1 min, 7 °C/min to 260 °C
FID flows: H_2 20 ml/min, air 400 ml/min, N_2 makeup 40 ml/min

Pentane (Sigma Aldrich, St. Louis, MO, USA) was used for the optimization of the modulator flush and fill times. Fragrance samples of Glade® scented oils (SC. Johnson, Racine, WI, USA) were used to evaluate the modulator and used without further dilution. The work with GasPro × Porabond Q columns was evaluated using a 1000 ppm C1–C6 alkane/alkene standard in nitrogen (Scott Specialty Gases, Plumsteadville, PA, USA).

In each case of comparison between forward flush and reverse flush, the fill and flush times were systematically varied to find the optimum conditions prior to comparison.

3. Results/discussion

3.1. Comparison of reverse and forward fill/flush modulation

Schematically the reverse fill/flush (RFF) modulator is shown in the fill state, Fig. 2A, and the flush state, Fig. 2B. The aim of reverse flush modulation is to minimize unmodulated effluent from the first column transferring to the second dimension during the fill cycle, the majority of the second dimension modulation period. The purpose of the bleed capillary is to provide an outlet for the carrier gas passing through the accumulation capillary during the fill cycle, and to allow a reversal of flow direction during the flush cycle. The other feature of reverse flush modulation is that when it is partially filled using a shorter fill cycle it can be flushed in a shorter period of time. The length and diameter of the bleed capillary is chosen to match the pressure/flow conditions of columns used – to provide flow equivalent to the output of the first dimension. The head pressure of the second dimension column was used with the Agilent pressure/flow calculator to determine the length of 0.1 mm ID capillary necessary to deliver 0.8 ml/min. For the 5 m × 0.25 mm ID second dimension column, a 3.2 m × 0.1 mm ID uncoated capillary was used as the bleed, connected to a second FID.

In forward flush/fill (FFF) modulation, during the flush state, flow from the first column continues to fill the accumulation capillary behind the portion being swept. This happens even under optimized conditions, if the first dimension flow is not stopped by a pressure pulse. If a component elutes from the first dimension while flushing the accumulation capillary, as the modulator returns to the fill state, that portion of the component will be more slowly transferred to the second dimension, resulting in tailing. This is very apparent when the modulator is not swept completely – either with an insufficient flow rate or flush time. In that case when a peak elutes, the signal does not completely return to baseline between modulations. Note that the observation of this phenomenon is most evident with high concentration components and can be masked by the scaling factors chosen for a plot. Under many analysis conditions this effect is not significant if even noticeable, provided that adjacent peaks in the second dimension do not differ widely in concentration. The peak tailing will also be a function of the flow ratio between the first and second dimension columns. As noted by Harvey and Shellie [17] there are several ways to achieve higher flow ratios. One alternative is to operate the second dimension at higher flow/pressures, giving up efficiency in the second

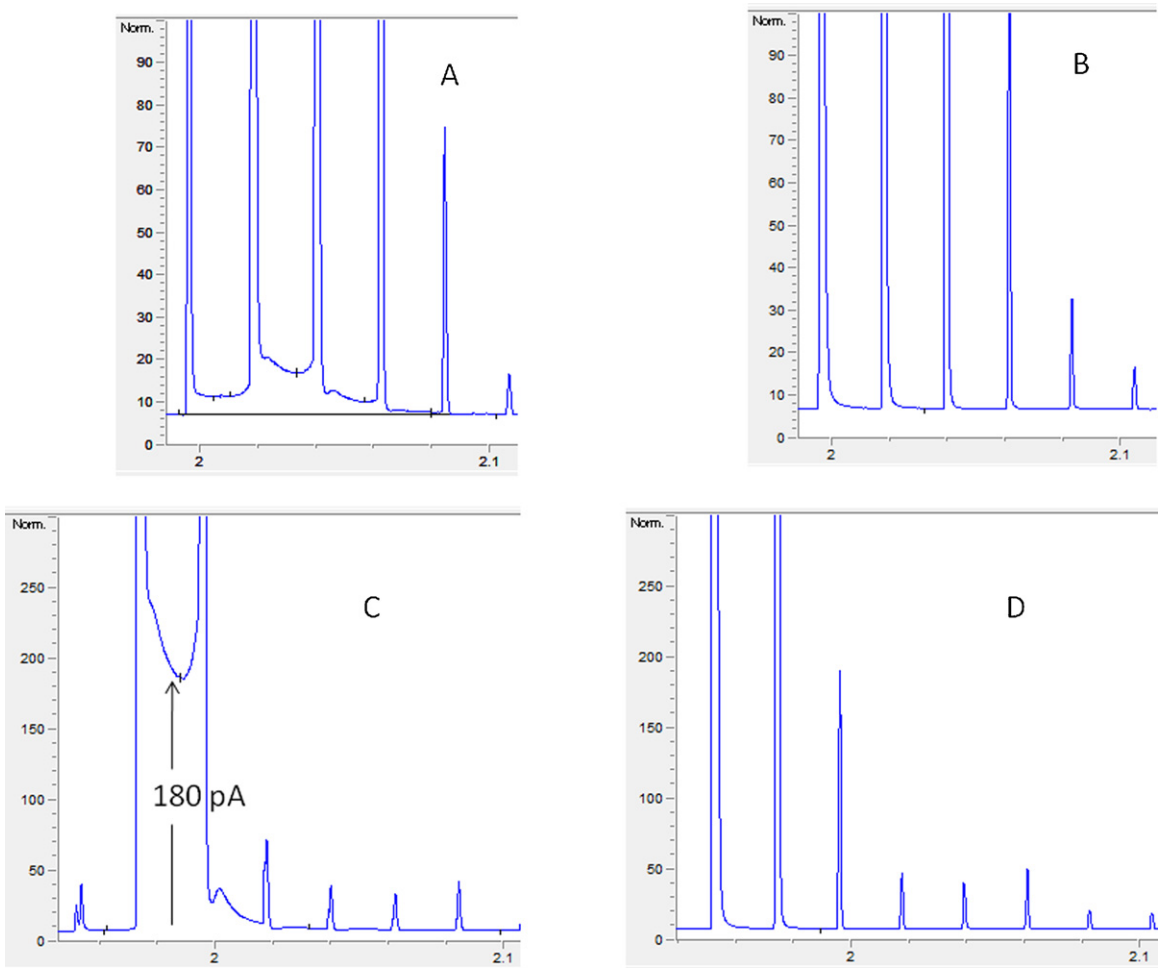

Fig. 3. (A) FFF modulation, pentane vapor, 1 μl injected at 20/1 split. (B) RFF modulation, pentane vapor, 1 μl injected at 20/1 split. (C) FFF modulation, pentane liquid, 0.1 μl injected at 200/1 split (baseline rise of 170 divided by height of 80,000 = 0.2%). (D) RFF modulation, pentane liquid, 0.1 μl injected at 200/1 split.

dimension. Another is to operate the first dimension column at suboptimal linear velocities.

Note that our approach to ensuring a complete return to baseline between modulations is quite different from Harvey et al. [18], where they used pressure restriction at the end of the first dimension column to stop the first dimension flow during the flush cycle and lengthen the time of the modulation cycle. In the work by Tranchida [14] this peak tailing should be reduced because of the ability to increase the ratio of second dimension flow to first dimension flow but this comes at the expense of sensitivity – sending a portion of the second dimension flow to waste.

3.2. Comparison of peak widths and symmetry

Pentane was injected over a range <1 ng to 30 μg to compare the two modulation methods. To cover this range both liquid and vapor injections were used. Representative chromatograms are shown in Fig. 3A–D. There is a very obvious difference in the return to baseline between the two types of modulation. It is also apparent that the baseline rise between modulations is dependent on the amount of the component injected. Peak statistics were calculated with GC-Image to quantify this difference as tabulated in Table 3. Some of the statistics such as symmetry are calculated for both the first and second dimension and are designated by the "I" or "II", respectively. All statistics are calculated as pixel units except for Variance. The Peak Value is equivalent to the peak maximum value (height). Volume is the integrated volume under the two-dimensional peak (blob). Eccentricity is the square of the difference between first and second dimension variance. Inertia is simply the sum of the first and second dimension variance. Orientation is a measure of the angular rotation of the elliptical blob due to simultaneous peak skewing in both dimensions. Variance is calculated from the square of the peak width and normalized by the Peak Volume. Skewness is a measure of asymmetry based on the third-order moments, normalized by the volume, center-of-gravity, and standard deviation. Symmetry, symmetry (50.0) and symmetry (10.0) are measures of the degree to which the peak apex has shifted off of the center of gravity as

Table 3
Comparison of peak statistics for pentane for FFF and RFF modulation.

Modulator	FFF	RFF	FFF	RFF
Approx Amt injected (ng)	300 (liq)	300 (liq)	15 (vap)	30 (vap)
Peak value	80,099	116,141	5216	12,575
Volume	1,041,497	1,181,516	115,311	283,474
Eccentricity	129,285	345	3490	666
Inertia	360	19	60	27
Orientation	0.0087	−0.0329	0.0208	−0.0272
Skewness II	−1.6	2.2	−2.8	3.9
Symmetry I	1.6	2.3	1.3	1.5
Symmetry II	2.6	7.3	3.9	8.1
Symmetry II(50.0)	77.29	0.78	49.36	0.85
Symmetry II(10.0)	24.0	1.5	26.3	1.1
Variance I (min-sqr)	1.4E-04	7.0E-05	3.3E-04	3.3E-04
Variance II (sec-sqr)	0.00900	0.00047	0.00149	0.00066

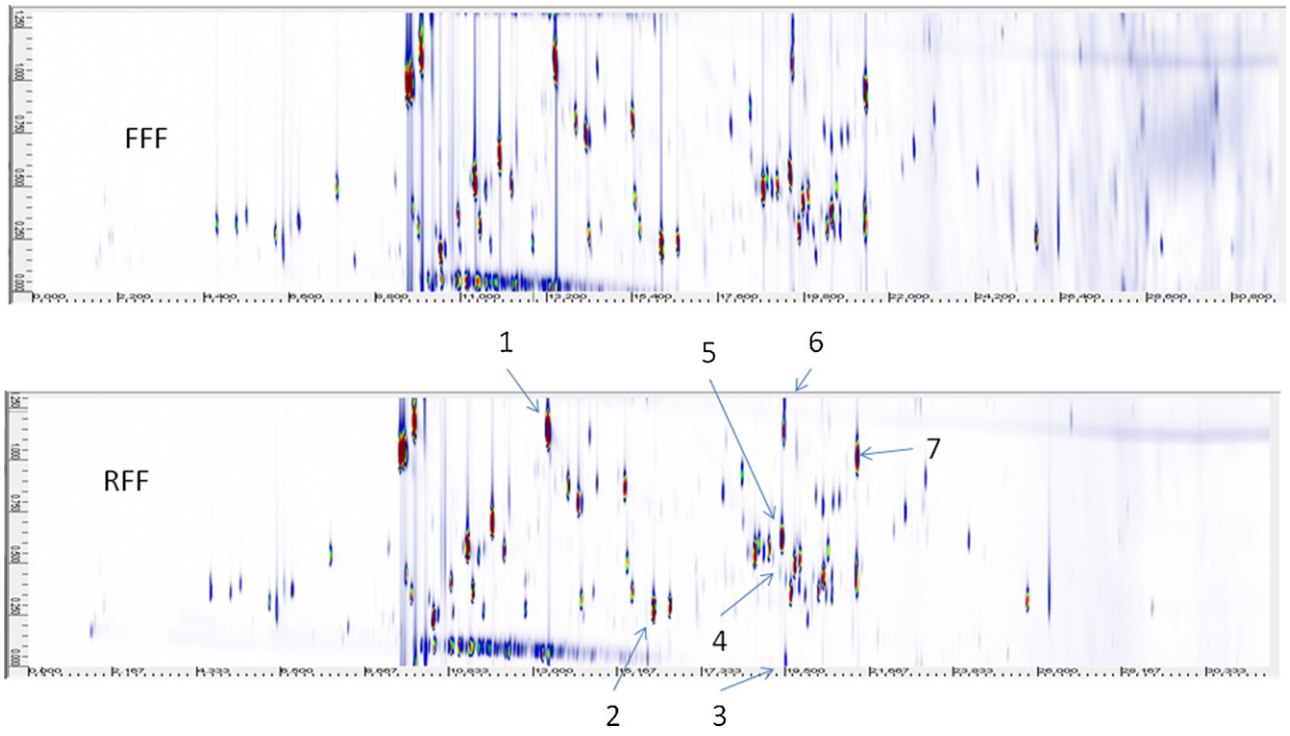

Fig. 4. Analysis of Glade® ocean blue scented oil, with peaks designated for precision study and overloading (1) acetic acid methylphenyl ester, (2) hexen-1-ol, acetate(E), (3) ethyl vanillin, (4) 3,7,7-trimethyl-1,3,5-cycloheptatriene, (5) 7 methoxymethyl-2,7-dimethyl -1,3,5-cycloheptatriene, (6) 2(3H)-furanone, 5-hexylhydro, (7) 5-heptylhydro-2(3H)-furanone.

measured at the baseline, 50% and 10% of the height, respectively. Detailed definitions are available from Zoex Corporation [19].

Among the statistics that are calculated based on both the first and second dimension, Eccentricity is the most sensitive to the difference between FFF and RFF modulation. Symmetry should be very sensitive to peak tailing calculated for the second dimension. But if a peak tails in the second dimension longer than one modulation period, GC-Image cannot reliably assign the start and end of the peak in the second dimension. Thus, the symmetry II values in Table 3 do not show a clear difference between FFF and RFF modulation. Symmetry II (50.0) and symmetry II (10.0) do show a clear difference but this is due to the differences of the peak width and not a measure of the baseline rise between modulations. The same effect is seen in the variance values. Though the peak statistics calculated for the second dimension show an improvement with RFF modulation, as multiple chromatograms were examined it became apparent that many of the common peak statistics such as symmetry, skewness and peak tailing factor are not consistently sensitive to tailing that occurs below well below 1% of the peak height. For example the USP peak-tailing factor is calculated at 5% of the peak height. This is completely inadequate to detect the streaking that commonly is observed in GC × GC. Measurements of skewness using GC-Image have shown correlation with "streaking" in the second dimension but these values are not intuitively obvious as to how they relate to a peak returning to baseline in the second dimension. For both 1D and 2D measurements of peak statistics, peak detection settings can play a significant role in the values obtained.

3.3. Intermodulation tailing factor

To make a more quantitative and more easily understood comparison of "streaking" in the second dimension we have defined a factor that is the difference between signal baseline and the valley of the two largest peak modulations, divided by the height of the largest modulation and multiplied 100 to give a percentage. This is illustrated for RFF and FFF modulation of pentane in Fig. 3A–D. The intermodulation-tailing factor as calculated for FFF modulation in 3C was 0.2%. This compares to 0.0002% for the RFF modulation in Fig. 3D. This would imply that components at concentrations below 0.2%, coeluting with the largest peak in the first dimension would be relatively difficult to quantify with FFF modulation. Since this was a relatively simple case, a more typical case encountered in industrial problem solving was chosen to evaluate the modulation methods to see if the same effect was observe with a wide range of components at different concentrations.

3.4. Overloading: effect of sample injection size

A fragrance sample was used to further investigate the impact of sample size on resolution in the second dimension. In Fig. 4, a comparison is shown between FFF and RFF modulation, with the specific components identified that were used in this study. Though there is a minor amount of streaking in both chromatograms, it is most apparent with components 1 and 2 that there is more streaking with FFF modulation. The amount of sample injected ranged from 0.5 to 50 μg at seven different levels to determine the impact on the separation quality. Since the most concentrated components, such as hexen-1-ol, acetate(E), are around 10% of the sample, the amount injected of the most concentrated components ranged from 50 to 5000 ng. To illustrate the improvement with RFF vs. FFF modulation a selected region of the two dimensional chromatogram was chosen at differing concentration levels where the largest peak eluting is hexen-1-ol, acetate(E), Fig. 5. At the lowest level injected, the FFF modulation shows a small amount of tailing. When the amount is increased to 500 and 5000 ng it is apparent that some components are not detectable until this amount of sample is injected. Note that nearly all of the components in this sample have wrapped around at least once. Also it is apparent that the largest peak, hexen-1-ol, acetate(E), is considerably overloaded in the first dimension.

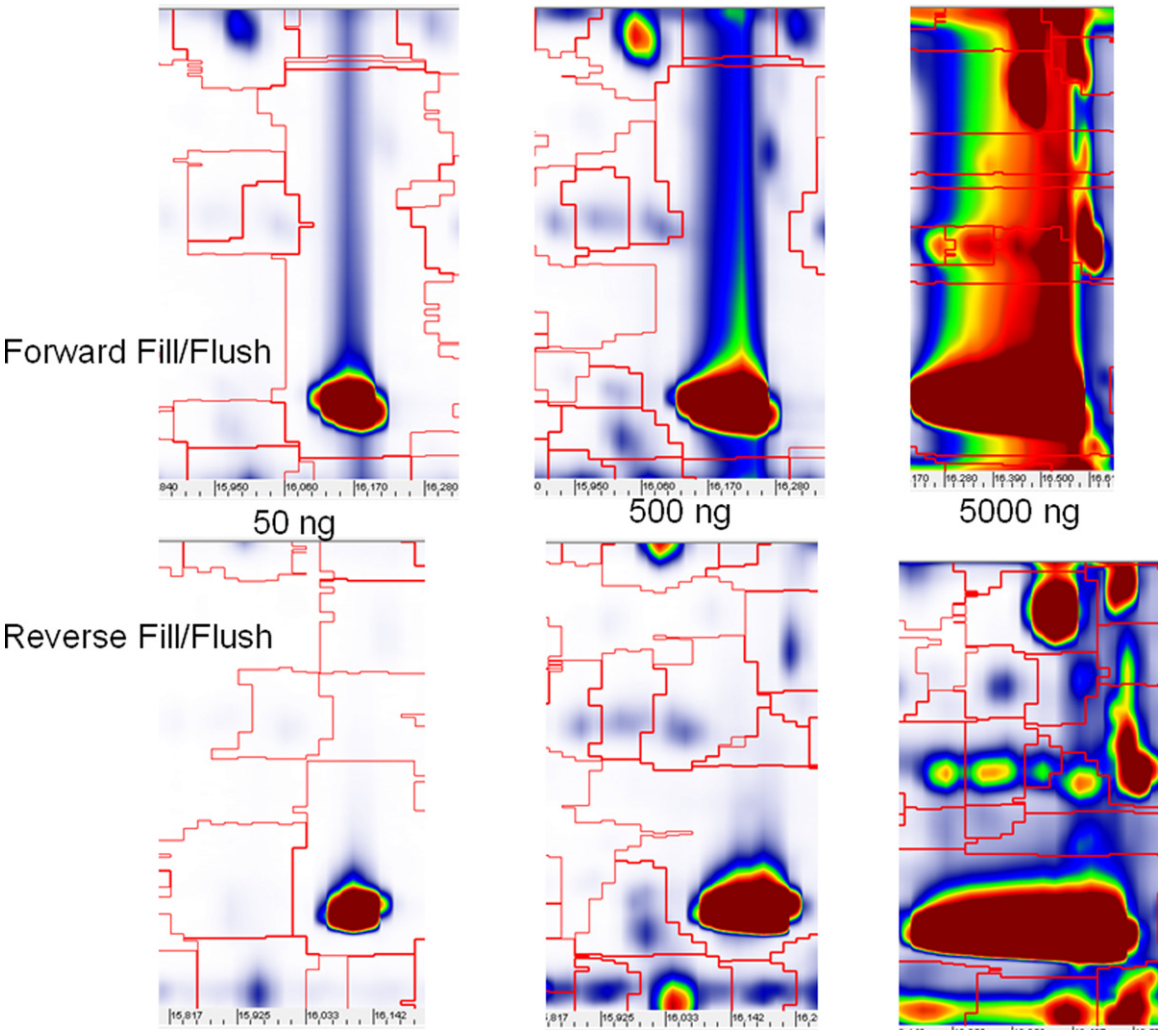

Fig. 5. Comparison of FFF modulation (top) vs. RFF modulation (bottom) with differing amounts of hexen-1-ol, acetate(E) injected.

However, this does not result in a significant loss of resolution in the second dimension for the chromatograms generated with RFF modulation. The second dimension column ID is typically equal to or larger than the first dimension in flow modulated GC × GC, thus overloading in the second should not typically be a problem. Whereas overloading in the second dimension is quite common in cryogenic modulation i.e., a 100 μm ID column is used as the second dimension coupled to a 250 μm ID column in the first dimension.

In Fig. 6 these same regions displayed in Fig. 5 are represented as a series of untransformed one-dimensional traces with two modulation cycles at the peak apex. Again the data show that with FFF modulation the detector signal does not completely return to baseline between modulations. This is due to the major component eluting from the first dimension into the modulator during the flush. When the modulator returns to the fill state, the accumulation capillary is not filled with pure carrier gas but rather a diluted concentration of the component from the first dimension (diluted by the flow ratio of the first to the second dimension, 0.8/20). To further quantify the difference, the baseline rise was measured for each amount injected, shown in Fig. 7, and intermodulation-tailing factor was calculated. For all FFF modulation levels measured the intermodulation tailing factor was slightly larger than 0.2%. For RFF modulation the intermodulation tailing factor was less than 0.01% for all but the highest level injected which was 0.016%. To make sure that this effect was not due to inadequate optimization, both modulation methods were optimized for first the fill and then the flush times. As expected, the optimum fill times were the same between both modulation methods because the same modulator tube (volume) was used. The flush time for FFF modulation was systematically varied in 0.01 s increments to verify both when the modulator was incompletely flushed (tailing peaks), to the extreme when the flush time was too long (fronting peaks). An important advantage of this system is that the second FID reveals clearly when the modulator is overfilled thus making it very straightforward to precisely set the fill time. Note that in this study optimization was not done by varying the flow of the second dimension because it would become much harder to compare chromatograms from the two modulation modes. This baseline rise between modulations was also observed when using the Agilent CFT modulator which operates in the FFF mode. The guidelines provided by Agilent were followed and the best results after optimization had an even higher baseline rise than the FFF results shown here. To verify that the observations were not specific to this type of sample, others were tested: FAMES, surfactants, olefin monomers, acrylate esters, and chlorinated hydrocarbons. All show the same phenomena when sufficient sample is injected i.e. 1 μl neat @ 20/1 split ratio. The obvious question is why this has not been observed in previous papers. The answer in part is that few publications on flow modulated

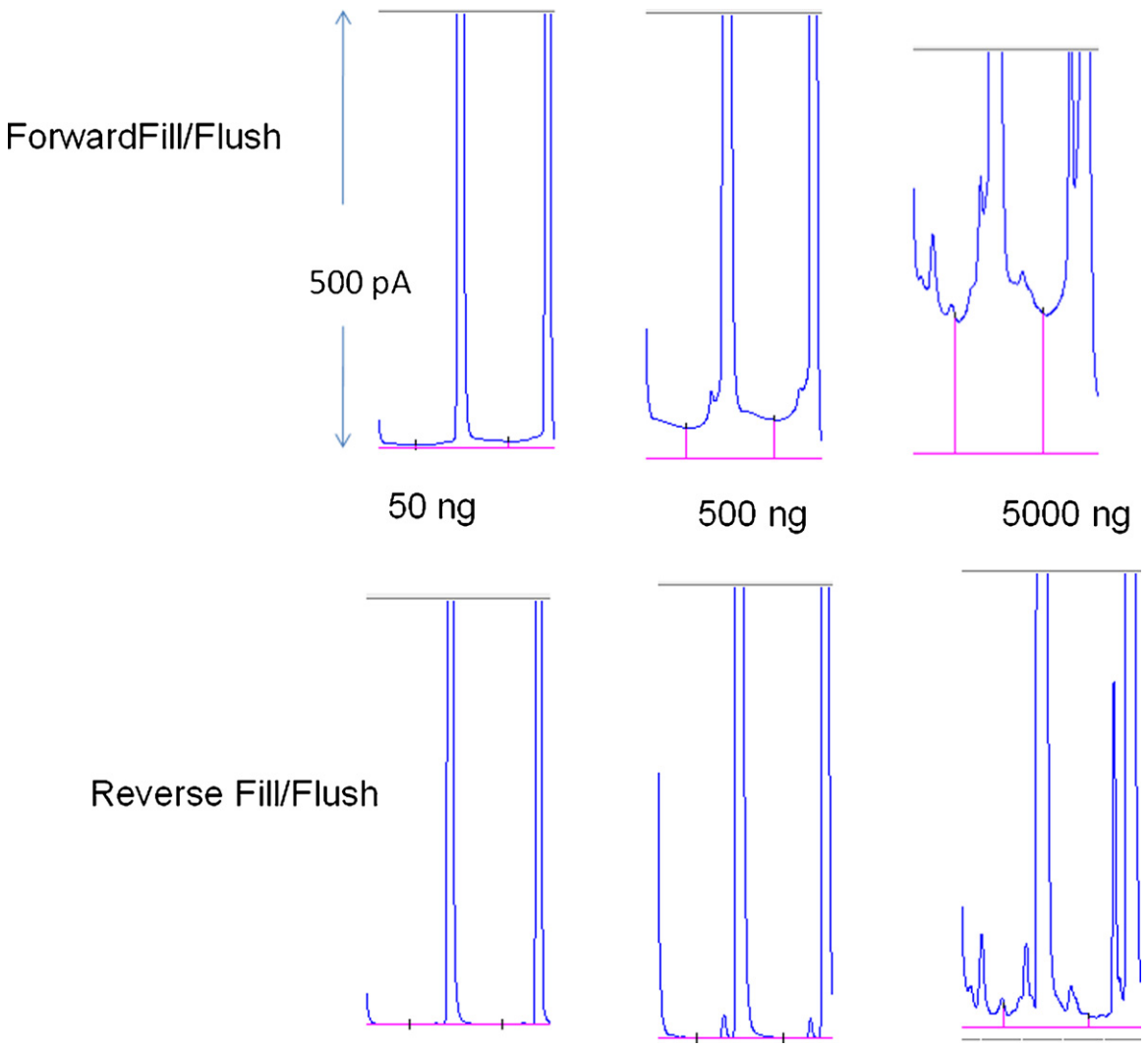

Fig. 6. Comparison of two modulation cycles with differing amounts of hexen-1-ol, acetate(E) injected.

GC × GC have focused on the issue of peak overload. Another reason is that overloading causes loss of resolution in the first dimension and that would not normally be recommended in a publication. It is also possible with the modified modulator proposed by Seeley that the insertion of the primary and secondary columns into the modulator provide a pressure restriction which slows or minimizes primary column flow during the flush step. As mentioned earlier, this has been demonstrated by Harvey as a way to stop the primary flow during the flush step and lengthen the modulation period.

3.5. Precision

To demonstrate the capability for quantitative analysis, 20 replicates of the scented oil sample were injected. Selected components, identified in Fig. 4, were quantified covering a range of concentrations. Components 3–6 were specifically chosen because they are resolved in GC × GC but completely overlapped in one-dimensional GC. The precision of analysis was better than 2% RSD for components that range from 0.1% to 10% in concentration. With forward flush/fill modulation, this analysis required manual reintegration of the components to get RSD's of 10–20%. In the case of the components shown in Fig. 5, quantitation was not possible at the highest amounts injected with FFF modulation due to loss of resolution.

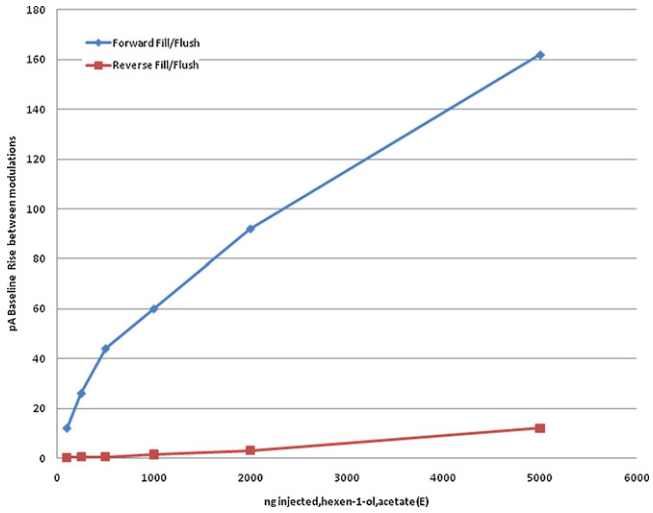

Fig. 7. Comparison of baseline rise between modulations of hexen-1-ol, acetate(E) for forward fill/flush vs. reverse fill/flush.

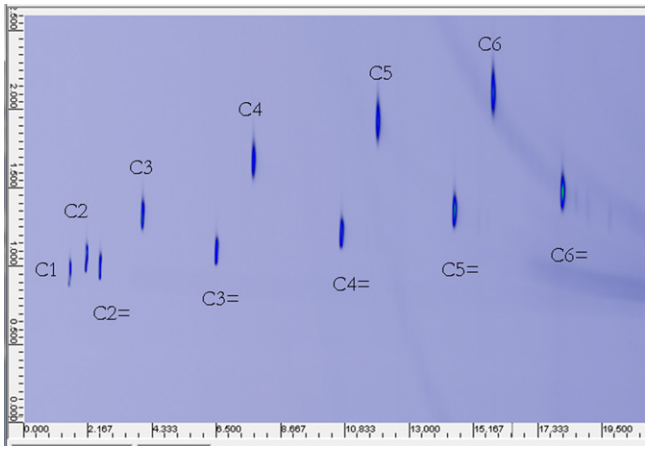

Fig. 8. Separation of C1–6 alkanes and alkene: GasPro in 1st dimension (50 °C, 1 min, 7 °C/min to 240 °C), Porabond Q in second dimension (70 °C, 1 min, 7 °C/min to 260 °C). Fill time 2.4 s, flush time 0.2 s.

3.6. Modulation of very light components

Flow modulation of permanent gases and light gases is easily done with flow modulation, but difficult to achieve with cryogenic modulation. Separation of very light components is difficult with WCOT columns and normally done with PLOT columns. PLOT columns exhibit unique selectivity, but are difficult to use with the same oven program for GC × GC. The selectivity is so different that at a given first dimension elution temperature either the *k* value in the second dimension is extremely low, resulting little second dimension separation or extremely large, causing wrap around. In Fig. 8 the separation of a series of C1–6 alkanes and olefins is demonstrated using a GasPro column (13.5 m × .25 mm ID) in the first dimension and a Porabond Q column (2 m × .25 mm ID) in the second dimension in a low thermal mass (LTM) module. Note that the length of the fused silica connections between the LTM, the modulator and the FID must be added to the second dimension column length for the 7890 GC to correctly calculate pressures required for constant flow operation. The bleed capillary was 1.75 m × 0.1 mm ID. In this case, the accumulation capillary volume was increased to 50 μl to give time for a longer modulation period. Because peaks are normally broader with PLOT columns, this can be done without under-sampling the first dimension. Similar performance was obtained with the Seeley modulator but as explained in the introduction, Vespel/graphite ferrules loosen with temperature cycling. The resultant leaks cause the baseline to rise and fall with each modulation.

4. Conclusions

This work has demonstrated an advance in performance for differential flow modulation. But there is still progress to be made in optimizing hardware to produce narrower bandwidths introduced to the second dimension. A simple and reliable differential flow modulator has been demonstrated, building on the original design of Seeley [4]. The modulator is constructed with commercially available capillary flow technology tees which simplifies set up and permits use of a wide range of column dimensions because the modulator volume is adjustable. Using a reverse fill/flush arrangement the baseline rise between modulations is substantially reduced as compared to forward flush modulation. Excellent precision has been demonstrated as well as the capacity to handle significant overloading without loss of resolution in the second dimension. This increases the effective peak capacity of flow modulated GC × GC.

Acknowledgements

The authors wish to acknowledge the many helpful discussions on this topic with Dr. John Seeley and Dr. Steven Reichenbach for assistance in evaluating data with GC-Image.

References

[1] P.A. Bueno, J.V. Seeley, J. Chromatogr. A 1027 (2004) 3.
[2] R.W. LaClair, P.A. Bueno, J.V. Seeley, J. Sep. Sci. 27 (2004) 389.
[3] N.J. Micyus, J.D. McCurry, J.V. Seeley, J. Chromatogr. A 1086 (2005) 115.
[4] J.V. Seeley, N.J. Micyus, J.D. McCurry, S.K. Seeley, Am. Lab. 38 (2006) 24.
[5] M. Kochman, A. Gordin, T. Alon, A. Amirav, J. Chromatogr. A1129 (2006) 95.
[6] J.V. Seeley, N.J. Micyus, S.V. Bandurski, S.K. Seeley, J.D. McCurry, Anal. Chem. 79 (2007) 1840.
[7] J.V. Seeley, S.K. Seeley, E.M. Libby, J.D. McCurry, J. Chromatogr. Sci. 45 (2007) 650.
[8] J.V. Seeley, E.M. Libby, S.K. Seeley, J.D. McCurry, J. Sep. Sci. 31 (2008) 3337.
[9] J.V. Seeley, S.K. Seeley, E.K. Libby, Z.S. Breitbach, D.W. Armstrong, Anal. Bioanal. Chem. 390 (2008) 323.
[10] M. Poliak, M. Kochman, A. Amirav, J. Chromatogr. A 1186 (2008) 189.
[11] Q. Gu, F. David, F. Lynen, K. Rumpel, G. Xu, P. De Vos, P. Sandra, J. Chromatogr. A 1217 (2010) 4448.
[12] G. Semard, C. Gouin, J. Bourdet, N. Bord, V. Livadaris, J. Chromatogr. A 1218 (2011) 3146.
[13] P. Manzano, E. Arnaiz, J.C. Diego, L. Toribio, C. Garcia-Viguera, J.L. Bernal, J. Bernal, J. Chromatogr. A 1218 (2011) 4952.
[14] P.Q. Tranchida, G. Purcaro, A. Visco, L. Conte, P. Dugo, P. Dawes, L. Mondello, J. Chromatogr. A 1218 (2011) 3140.
[15] P.Q. Tranchida, G. Purcaro, P. Dugo, L. Mondello, TrAC 30 (2011) 1437.
[16] L.M. Blumberg, J. Sep. Sci. 31 (2008) 3358.
[17] P.McA. Harvey, R.A. Shellie, J. Chromatogr. A 1218 (2011) 3153.
[18] P.McA. Harvey, R.A. Shellie, P.R. Haddad, J. Chrom. Sci. 48 (2010) 245.
[19] S. Reichenbach, Q. Tao, "GC × GC blob metadata and statistic in GC Image", white paper available from Zoex Corporation, Houston, TX or at www.zoex.com.